Pharmaceutical Research, Vol. 24, No. 10, October 2007 (© 2007)
DOI: 10.1007/s11095-007-9310-8

Research Paper

Preparation and Characterization of Innovative Protein-coated Poly(Methylmethacrylate) Core-shell Nanoparticles for Vaccine Purposes

Rebecca Voltan,[1] Arianna Castaldello,[1] Egidio Brocca-Cofano,[1] Giuseppe Altavilla,[2] Antonella Caputo,[1,6] Michele Laus,[3] Katia Sparnacci,[3] Barbara Ensoli,[4] Silvia Spaccasassi,[5] Marco Ballestri,[5] and Luisa Tondelli[5]

Received January 12, 2007; accepted April 4, 2007; published online May 3, 2007

Purpose. This study aims at developing novel core-shell poly(methylmethacrylate) (PMMA) nanoparticles as a delivery system for protein vaccine candidates.
Materials and Methods. Anionic nanoparticles consisting of a core of PMMA and a shell deriving from Eudragit L100/55 were prepared by an innovative synthetic method based on emulsion polymerization. The formed nanoparticles were characterized for size, surface charge and ability to reversibly bind two basic model proteins (Lysozyme, Trypsin) and a vaccine relevant antigen (HIV-1 Tat), by means of cell-free studies. Their *in vitro* toxicity and capability to preserve the biological activity of the HIV-1 Tat protein were studied in cell culture systems. Finally, their safety and immunogenicity were investigated in the mouse model.
Results. The nanoparticles had smooth surface, spherical shape and uniform size distribution with a mean diameter of 220 nm. The shell is characterized by covalently bound carboxyl groups negatively charged at physiological pH, able to reversibly adsorb large amounts (up to 20% w/w) of basic proteins (Lysozyme, Trypsin and HIV-1 Tat), mainly through specific electrostatic interactions. The nanoparticles were stable, not toxic to the cells, protected the HIV-1 Tat protein from oxidation, thus preserving its biological activity and increasing its shelf-life, and efficiently delivered and released it intracellularly. *In vivo* experiments showed that they are well tolerated and elicit strong immune responses against the delivered antigen in mice.
Conclusions. This study demonstrates that these new nanoparticles provide a versatile platform for protein surface adsorption and a promising delivery system particularly when the maintenance of the biologically active conformation is required for vaccine efficacy.

KEY WORDS: carboxyl groups; core-shell nanoparticles; poly(methylmethacrylate); proteins; vaccines.

INTRODUCTION

CD4+ and CD8+ T cells play an essential role in the control of viral infections and tumors (1–3). Thus, vaccine formulations which target professional antigen presenting cells and modulate processing and presentation of antigens to T cell may afford better and long-lasting protection against viruses and tumors (4–6). Soluble antigens (peptides, proteins and DNA) delivered by the systemic and mucosal routes are generally scarcely immunogenic due to their poor intracellular uptake and stability. Nevertheless, their co-administration with adjuvants/delivery systems greatly enhances their stability and immunogenicity, thus reducing the antigen dose required. Biodegradable microparticles have been successfully used as delivery systems of entrapped vaccines. However, following encapsulation and release, DNA and proteins may be unstable and easily degraded, leading to a significant reduction in vaccine activity (7,8). Thus, a novel approach has been described, where charged cationic or anionic molecules [e.g. cetyltrimethylammonium bromide (CTAB) and sodium dodecyl sulphate (SDS)] are adsorbed to the surface of nano- and micro-particle to provide functional groups able to interact with the DNA or proteins/peptides, leading to an increased potency of the vaccine activity (9–12). In these systems, however, the use of chlorinated solvents and high amounts of surfactants and/or detergents during particle preparation may affect their biocompatibility, in particular for the development of injectable formulations (13,14). Although inclusion of such compounds in vaccine adjuvants cannot be totally excluded, the development of surfactant free vaccine carrier may represent an advantage in the field.

[1] Department of Histology, Microbiology and Medical Biotechnology, Section of Microbiology, University of Padova, Via A. Gabelli 63, 35122 Padova, Italy.
[2] Institute of Pathologic Anatomy, University of Padova, Via A. Gabelli 63, 35122 Padova, Italy.
[3] Department of Life and Ambient Sciences (DISAV), University of Piemonte Orientale and INSTM, UdR Piemonte Orientale, Via Bellini 25/G, 15100 Alessandria, Italy.
[4] National AIDS Center, Istituto Superiore di Sanità, Viale Regina Elena 299, 00161 Roma, Italy.
[5] I.S.O.F., Consiglio Nazionale delle Ricerche, Via Piero Gobetti 101, 40129 Bologna, Italy.
[6] To whom correspondence should be addressed. (e-mail: antonella.caputo@unipd.it)

0724-8741/07/1000-1870/0 © 2007 Springer Science + Business Media, LLC

In the present study, polymeric core-shell nanoparticles (<300 nm) able to reversibly bind biologically active proteins on their surface without the need of surfactants and/or detergents have been designed for use as delivery systems for the development of systemic and/or a mucosal subunit vaccines against infectious agents or tumors. The particles have been synthesized by a hybrid particle forming procedure that involves an emulsion type-polymerization in which the conventional emulsifier agent is substituted by a polymeric electro-steric stabilizer, namely the commercially available acrylic copolymer Eudragit L100-55 (15). As a consequence, these nanoparticles possess a core-shell structure, with a core constituted by poly(methylmethacrylate) (PMMA) and a highly hydrophilic shell composed by Eudragit. In contrast to the previously described PLGA or wax particles (16–18), the preparation of the present core-shell nanoparticles, as well as of the corresponding vaccine formulations, does not require surfactants. In addition, their surface is inherently able to accommodate a protein. This novel structure avoids the physical desorption and/or instability/toxicity drawbacks associated with vaccine formulations containing free surfactants and/or detergents thus ensuring the generation of safe vaccine formulations able to bind antigens in a reproducible way.

Accordingly, the aim of the present study is the analysis of the physico-chemical properties of the described nanoparticles as concerned their ability to reversibly bind two basic, model proteins (Lysozyme, Trypsin). In addition, toxicity and preservation of biological activity of a vaccine relevant antigen (HIV-1 Tat) was studied in cell cultures, whereas *in vivo* safety and immunogenicity were investigated in mice. The results suggest that they represent a promising delivery system for vaccination with subunit vaccines, particularly when a native protein conformation is required.

MATERIALS AND METHODS

Synthesis of Core-shell Nanoparticles

Methylmethacrylate (99%) was purchased from Aldrich and was distilled under vacuum before use. Potassium persulfate (Aldrich, 98%) was used without further purification. Eudragit L100-55 (Röhm Pharma) is an anionic copolymer based on methacrylic acid and ethyl acrylate, with a 1:1 ratio of the free carboxyl groups to the ester groups and an average molecular weight of approximately 250.000 g mol $^{-1}$. It has a pH-dependent solubility and is readily soluble in neutral to weakly alkaline conditions.

The MA7 nanoparticle sample was prepared according to the following procedure. In a 1 l five-neck reactor equipped with a condenser, a mechanical stirrer, a thermometer and inlets for nitrogen and containing 500 ml of deionized water, 2.0 g of Eudragit L100-55 and 10 ml of 1 M NaOH were introduced at room temperature with a stirring rate of 300 rpm. The mixture was purged with nitrogen and nitrogen was fluxed during the entire polymerization procedure. The mixture was then heated to 80°C and methylmethacrylate (175 ml, 1.636 mol) was added. After additional 15 min equilibration time, a potassium persulfate aqueous solution (10 ml, 62 mg) was added and the mixture was reacted for 24 h. At the end of the reaction, the product was filtered and purified by diafiltration using an Amicon 8400 stirred cell equipped with ultrafiltration biomax-500 membranes (cut off of 500 kDa). The diafiltration was performed with water until no residual monomer, as determined by gas chromatography (GC), or Eudragit, as determined by high-pressure liquid chromatography (HPLC), were detected. After this procedure, the polymeric nanoparticles were dried under vacuum at room temperature. Nanoparticle yield was estimated as the ratio between the final nanoparticle and the initial monomer weights and resulted 67%. Because of the relatively low yield some residual monomer was found in the raw material at the end of the reaction, but it was completely eliminated by the diafiltration as determined by GC. The amount of Eudragit L100-55 linked to the nanoparticles surface was determined by back titration of the excess NaOH after complete reaction of the acid groups and nanoparticles removal by centrifugation. To this purpose, 0.6 g of the nanoparticle sample were dispersed in 10 ml of 20 mM NaOH at room temperature for 24 h. Then, the nanoparticle sample was collected by centrifugation and washed twice with 25 ml of distilled water. The supernatants were combined and the excess NaOH was titrated with 20 mM HCl. The amount of NaOH which reacted with the surface bound Eudragit was then estimated by difference with the amount of free NaOH.

The MA7 nanoparticles can be lyophilized and stored in a powder form for at least 36 months and resuspended under stirring in aqueous solutions (water, 20 mM phosphate buffer, PBS etc.). Alternatively, they can be stored in concentrated aqueous suspensions (5–20 mg/ml) at 4°C or room temperature without affecting their physico-chemical properties.

Finally, sample SA7 was prepared according to the same experimental procedure described for sample MA7 but without the Eudragit. Nanoparticle yield was 73%.

Particle Size, Morphology and ζ-potential Measurements

Nanoparticles size and size distribution were measured by a JEOL JSM-35CF scanning electron microscope (SEM) with an accelerating voltage of 20 kV. The samples were sputter coated under vacuum with a thin layer (10–30 Å) of gold. The magnification is given by the scale on each micrograph. The SEM photographs were digitalized, using the Kodak photo-CD system, and elaborated by the NIH Image (version 1.55, public domain) processing program. From 150 to 200 individual nanoparticle diameters were measured for each optical micrograph. Photon Correlation Spectroscopy (PCS) measurements were run in water (HPLC grade) containing 10 mM NaCl on a Malvern Zetasizer 3000 HS instrument, at a scattering angle of 90° at 25°C. Each nanoparticle preparation (20 μg/ml) was analyzed with 10 readings per sample. ζ-potential measurements were carried out at 25°C on a Malvern Zetasizer 3000 HS instrument, after dilution of nanoparticles in water. All measurements were run in triplicate.

Proteins and Peptides

Trypsin and Lysozyme proteins were purchased from Sigma. The biologically active Tat protein (86 aa) of HIV-1 (HTLVIII-BH10) was produced in *Escherichia coli*, purified as a good laboratory practice (GLP) manufactured product, tested for activity as previously described (19), and provided by Diatheva (Fano, Italy). To prevent oxidation (due to the presence of seven cysteines in Tat protein sequence), the Tat

protein was stored lyophilized at −80°C and resuspended (2 mg/ml) in degassed commercial phosphate buffered saline (PBS) immediately before use (19). In addition, since Tat is photo- and thermo-sensitive, the handling of Tat was performed in the dark and on ice. Experiments were also performed with Tat oxidized by exposure to light and air for 16 h. By this procedure, Tat loses its biological activity due to conformational changes, including multimerization and aggregation of the protein with loss of the monomeric active form (19–21). Endotoxin concentration of different GLP lots of Tat, Trypsin and Lysozyme was below the detection limit (<0.05 EU/μg), as tested by the *Limulus* Amoebocyte Lysate analysis. The VCF (VCFITKALGISYGRK) Tat peptide containing a K^d-restrict CTL epitope and a CD4+ T cell epitope (22) was synthesized by UFPeptides s.r.l. (Ferrara, Italy), resuspended in H_2O (10^{-2} M) and stored at −80 C.

Cell-free Adsorption/release Experiments

Trypsin and Lysozyme adsorption/release behaviour was investigated on the MA7 nanoparticle sample. For binding experiments, nanoparticles (1–5 mg/ml) were incubated in 1 ml of 20 mM sodium phosphate buffer solution (pH 7.4) in the presence of increasing protein concentration (10–500 μg/ml) for 2 h at room temperature. Then, the nanoparticle/protein complexes were collected by centrifugation at 18,000 rpm for 10 min and the amount of the residual protein in the supernatant (unbound protein) was estimated using the bicinchoninic acid (BCA) protein assay (23). The amount of adsorbed protein and the efficiency of adsorption were calculated as the difference between the fed and the residual protein. The reported results are the mean of three independent experiments.

For protein release experiments, the nanoparticle/protein complexes were prepared as described above, washed twice with 1 ml of water, and then incubated at 37°C in 1 ml of 20 mM phosphate buffer containing 1 M NaCl. The amount of desorbed protein was measured by means of BCA colorimetric method. The amount of released protein, measured after 10, 30, 60 and 120 min, was maximum after 30 min (data not shown), therefore 30 min was chosen as incubation time for release experiments described in the results section. The effect of salt concentration on binding/release efficiency was measured using 1 ml of 20 mM phosphate buffer (pH 7.4) added with increasing concentrations of NaCl (0–1 M). To investigate the effect of pH variation on binding/release efficiency, buffers with different pH values were prepared by adding increasing amount of 0.2 M NaOH (buffer B) to 0.03 M citric acid, 0.03 M potassium phosphate, 0.03 M boric acid (buffer A). The reported results are the mean of three independent experiments.

To determine the binding of HIV-1 Tat protein, MA7 nanoparticles were resuspended at 1 mg/ml in PBS and incubated (50 μl) with increasing doses of Tat (1, 2, 5 and 10 μg) (corresponding to 0.02–0.2 mg of Tat/mg of nanoparticles/ml) under continuous stirring. To reduce the risk of Tat oxidation, incubation was run for 1 h at 4°C (instead of 2 h at room temperature as done for cell-free binding experiments with Trypsin and Lysozyme), as reduction in both temperature and time incubation do not affect Tat adsorption (data not shown).

The Tat/MA7 complexes were collected by centrifugation at 15,500 rpm for 15 min and to determine the amount of Tat protein bound to the particles surface, the complexes were dissociated and analyzed as follows: the Tat/MA7 complexes were resuspended in 15 μl of loading buffer (0.5 M Tris/HCl, pH 6.8, 2% SDS, 4% beta-mercapto-ethanol and Bromophenol-Blu), boiled for 5 min and spun again to separate MA7 particles (pellet) from Tat (supernatants). Supernatants, corresponding to bound Tat, were then run onto 15% SDS-PAGE and stained with Coomassie blue. Increasing doses of Tat protein (1, 2, 5 and 10 μg) were run in each gel as standard curve. Gels were analysed with the GelDoc Quantity One System (BioRad), and the amount of Tat recovered after boiling was determined by linear regression analysis on the Tat standard curve included in each gel. The percentage (%) of binding was determined for each binding dose as (μg of recovered Tat/μg of added Tat) × 100. The reported results are the mean (± SEM) of three independent experiments.

Cell Cultures

Monolayer cultures of HL3T1 cells, a human epithelial (HeLa) cell line containing an integrated copy of the chloramphenicol acetyl transferase (CAT) bacterial reporter gene under the HIV-1 long-terminal repeat (LTR) promoter, were obtained from NIH AIDS repository and grown in Dulbecco's minimal essential medium (DMEM; Cambrex, Bergamo, Italy) containing 10% heat-inactivated fetal bovine serum (FBS; Hyclone, Logan, UT). In these cells CAT gene expression occurs only in the presence of biologically active Tat protein (either added as exogenous protein or endogenously expressed after *tat* gene transfection) and it is a dose-dependent effect. Monocytes-derived dendritic cell (MDDC) cultures were obtained from purified human peripheral blood mononuclear cells (PBMC) by granulocyte-macrophage stimulating factor (GMCSF) and interleukin-4 (IL-4) stimulation, and characterized by fluorescent-activated cell sorter (FACS) analysis, as previously described (21).

Analysis of *in Vitro* Cytotoxicity

HL3T1 cells (4×10^3/100 μl) and MDDC (2×10^5/100 μl) were seeded in 96-well plates and cultured at 37°C for 24 h. One hundred microliters of medium containing increasing concentrations of MA7 nanoparticles alone (10–500 μg/ml) or bound to Tat (1 μg/ml) were then added to the cells in sestuplicate wells. MA7/Tat complexes were prepared following incubation of the appropriate volumes of MA7 and Tat. Since the adsorption efficiency of Tat on MA7 nanoparticles is the same at 4 and 25°C, in these experiments the two components were incubated for 1 h at 4°C, to reduce the risk of Tat oxidation. The complexes were then collected by centrifugation at 15,500 rpm for 15 min, resuspended in the appropriate volume of degassed sterile PBS and added to the cells immediately. Untreated cells and cells cultured in the presence of Tat alone (1 μg/ml) were the controls. After 96 h at 37°C, cell viability was measured using the colorimetric cell proliferation kit (MTT-based) provided by Roche (Roche, Milan, Italy). Absorbance values were measured by reading the plates at 570 nm with reference wavelength at 630 nm (OD 570/630). Percentage (%) of cell viability was determined as (OD of treated cells/OD of untreated cells) × 100. The reported results are the mean

(± SEM) of three independent experiments. One-way Anova followed by Dunnett's multiple comparison post-test were used for statistical comparison of each dose versus the control.

CAT Assays

Increasing doses of Tat (0.125, 0.5, 1 μg) were incubated with the same dose (30 μg) of MA7 nanoparticles (resuspended in PBS at 2 mg/ml) under continuous stirring for 1 h at 4°C. After incubation, Tat/MA7 complexes were collected at 15,500 rpm, resuspended in 15 μl of degassed sterile PBS, and immediately added to HL3T1 cells (5×10^5/ml) in 6-well plates in the presence of 100 μM chloroquine. Cells incubated with Tat alone were the controls. In some experiments, Tat and Tat/MA7 complexes were exposed to light and air at room temperature for 24 h (oxidation treatment) before addition to the cells. After 48 h incubation at 37°C, CAT activity was measured in cell extracts, as previously described (24). The percentage of CAT activity was calculated by the formula (cpm of acetylated ^{14}C-chloramphenicol/total cpm of acetylated and unacetylated ^{14}C-chloramphenicol) × 100. Finally, in some experiments, Tat and Tat/MA7 complexes were prepared, divided in three samples, one of which was immediately added to the cells ($t=0$) and the others stored at 4 or 25°C for 28 days ($t=28$ days) before addition to the cells. After 48 h incubation at 37°C, CAT protein expression (ng/mg of total proteins) was measured in cell extracts using a colorimetric enzyme-linked immunosorbent assay (ELISA) (Roche), according to the manufacturer's instructions. The reported results correspond to the mean of three to six independent experiments (± SEM). Two-way Anova and Bonferroni post-test were used for statistical comparison of each sample versus cells incubated with Tat alone.

Mice Studies

Animal use was according to national guidelines and institutional policies. To determine the safety of MA7 *in vivo*, female BALB/c mice of six to eight weeks of age (Charles River, Italy) were inoculated with 30 μg of MA7 alone or complexed with 1 μg of Tat. Mice were inoculated with 100 μl intramuscularly (i.m.) in the posterior quadricep muscles (50 μl/leg) at weeks 0 and 4, or with 10 μl intranasally (i.n.) (5 μl/nostril) at days 0, 7, 14, and 21. During the experiments, animals were controlled twice a week at sites of injection and for their general conditions (such as liveliness, food intake, vitality, weight, motility, sheen of hair). Ten to 15 days after the last inoculum mice were anesthetized intraperitoneally with 100 μl of isotonic solution containing 1 mg of Zoletil (Virbac, Milan, Italy) and 200 μg Rompun (Bayer, Milan, Italy), sacrificed and subjected to autopsy. Sample of cutis, subcutis and skeletal muscles at the site of injection and other organs (lungs, heart, intestine, kidneys, brain, liver, spleen and draining lymph nodes) were collected and processed for histological, histochemical and immunohistochemical examination, as described previously (25,26). For immunogenicity studies, groups of mice ($n=5$) were inoculated i.m. as described above, and control mice were inoculated with Tat alone (1 μg) or PBS. Mice were sacrificed 15 days after the last inoculation to collect blood and spleens for analysis of immune responses.

Analysis of Immune Responses

Splenocytes were purified from spleens squeezed on filters (Cell Strainer, 70 μm, Nylon, Becton Dickinson). Following red blood cell lysis with RBC lysing buffer (Sigma, Milan, Italy), cells were washed with RPMI 1640 containing 10% FBS (Hyclone), spun for 10 min at 1,200 rpm, resuspended in RPMI 1640 containing 10% FBS, 1% L-glutamine (BioWhittaker, Walkersville, MD), 1% penicillin/streptomycine (BioWhittaker, Walkersville, MD), 1% non essential aminoacids (Sigma), 1 mM sodium piruvate (Sigma) and 50 mM β-mercaptoethanol (Gibco, Grand Island, NY), and used for the analysis of cellular immune responses (22). Cellular responses were analyzed using pools of spleens per experimental group.

Proliferation assays were performed in sestuplicates using 2×10^5 cells/200 μl/well (round-bottom plates, NUNC) as previously described. The reported results are expressed as stimulation index (S.I.) determined as the ratio between the mean counts/minute of antigen-stimulated wells and the mean counts/minute of the same unstimulated sample.

Enzyme-linked immunospot (Elispot) assays were performed in duplicate wells for Th1 (INF-γ, IL-2) and Th2 (IL-4) cytokines on freshly isolated splenocytes stimulated for 16 h with the VCF Tat peptide, using commercially available murine INF-γ, IL-2 and IL-4 Elispot kits (BD, Pharmingen), as previously described (22). Results are expressed as number of spot forming cells (SFC)/10^6 cells. Responses at least 2-fold higher than the mean number of spots in the control wells and ≥30 were considered positive.

IgG end point titers were measured by ELISA, as previously described (27). The reported results are the reciprocal log of the arithmetic mean endpoint titers (± SEM) of mice sera tested individually.

RESULTS

Synthesis of Core-shell Nanoparticles

The MA7 sample was prepared following an innovative single step hybrid particle forming procedure which involves an emulsion type-polymerization in which the conventional emulsifier agent is substituted by a polymeric electro-steric stabilizer. In these conditions, core-shell nanoparticles with very homogeneous size and size distribution were generated. In addition, the electrosteric stabilizer at the end of the reaction is located at the nanoparticle surface and affords functional groups able to interact with proteins (15). SEM analysis of the MA7 sample (Fig. 1) showed a monomodal diameter distribution with mean diameter value of 220 ± 8 nm.

To get information about the nanoparticle surface nature, sample SA7 was prepared according to the same experimental procedure described for sample MA7 but without the Eudragit. SA7 is characterized by an average diameter of 530 nm, which is larger than MA7 particles diameter because Eudragit provides an additional contribution to the particle stabilization during the emulsion polymerization process. In the absence of Eudragit, the stabilization is afforded only by the

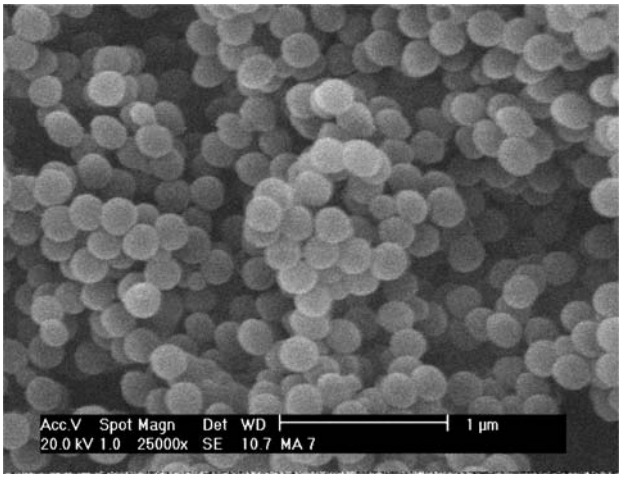

Fig. 1. SEM micrograph of MA7 core-shell nanoparticles.

ionic species formed in water from initiator decomposition and monomer addition, in agreement with the usual emulsifier free emulsion polymerization process mechanism. Figure 2 illustrates the trend of the ζ-potential for both nanoparticle samples, MA7 and SA7, as a function of pH. The ζ-potential of SA7 is negative, as a result of the presence of anionic groups deriving from initiator fragments, and pH insensitive. In contrast, the ζ-potential of MA7 is negative and decreases with a typical sigmoidal shape as the medium pH increases. The same figure illustrates the Eudragit ionization degree as a function of pH. The striking relation between the Eudragit ionization degree and the MA7 ζ-potential is a clear proof of the presence of Eudragit at the surface. The amount of Eudragit was determined by acid-base titration and the amount of carboxyl groups on the nanoparticle surface is 6.430×10^{-5} mol of carboxyl groups/g. The MA7 nanoparticle sample was also subjected to a procedure consisting of a neutralization step, dialysis, re-acidification and dialysis again. This cycle was repeated four times and at the end of each cycle the amount of Eudragit was determined. Within the experimental error, the amount of Eudragit remained constant, thus indicating that the Eudragit is tightly linked to the nanoparticle surface.

Physico-chemical Characterization

The behaviour of free MA7 nanoparticles in physiologically relevant buffers was studied by means of dynamic light scattering techniques. Photon correlation spectroscopy (PCS) measurements run in the presence of increasing NaCl concentration demonstrated that aqueous suspensions of MA7 nanoparticles are stable up to 0.5 M salt concentration without showing any aggregation effect. In particular, the hydrodynamic diameter increased from 249.2 to 337.8 nm (36%) in the salt concentration range comprised between 0.01 and 0.5 M, whereas the ζ-potential value gradually decreased from −48.3 to −5.5 mV. In addition, both PCS size and electrophoretic mobility of aqueous suspensions of free nanoparticles were not affected by pH variation ranging from 6 to 10. On the contrary, an acid environment ($3<pH<6$) promoted a strong increase of the ζ-potential value towards zero and an increase of PCS diameter, as protonation of carboxyl surface groups reduces the effect of electrostatic repulsion and promotes particle aggregation.

Analysis of Protein Binding and Release

To test the binding/release ability of the core-shell carboxylated nanoparticles, the MA7 sample was resuspended at 5 mg/ml concentration in 20 mM phosphate buffer (pH 7.4) and incubated with increasing amounts [from 10 to 500 µg/ml, i.e. 0.2–10% protein/particle ratio (w/w)] of two model basic proteins, namely Trypsin (MW=23.783 Kda) and Lysozyme (MW=18.656 Kda), whose isoelectric points are 9.64 and 10.11, respectively. Under these experimental conditions, the MA7 nanoparticles adsorbed Lysozyme with 100% efficiency up to 300 µg/ml protein concentration and with approximately 90% efficiency in the presence of higher protein concentration (data not shown). Conversely, the adsorption efficiency of Trypsin was 100% only at low protein concentration (10 µg/ml) and it slightly decreased (70%) in the 100–500 µg/ml protein concentration range (i.e 2–100 µg/mg). Thus, as a result of the binding affinity, the amount of protein that can be adsorbed on these nanoparticles ranges from 2 up to approximately 70–90 µg/mg, i.e. 7–9% w/w (Fig. 3a). Under the same experimental conditions, adsorption of proteins with lower isoelectric point (i.e. Pepsin) occurred to a very low extent (L. Tondelli, personal communication), thus indicating that the carboxylated MA7 nanoparticles specifically bind basic proteins.

As at 5 mg/ml nanoparticles concentration no saturation of functional surface was observed, binding experiments with higher protein/particle ratio were also run. To this purpose, the particle loading ability was tested at 1 mg/ml of nanoparticles concentration with increasing doses of Lysozyme or Trypsin (from 10 to 500 µg/ml, i.e. 1–50% w/w). Both proteins showed a strong increase in the final loading values, up to 150–200 µg/mg, i.e. 15–20% w/w (data not shown), which are considerably higher as compared to those described in the literature (14,28–30). It is noteworthy that protein adsorption is a highly reproducible and efficient process with both proteins. In addition, protein adsorption efficiency seems to be strictly dependent on the intrinsic physico-chemical and conformational properties of the pro-

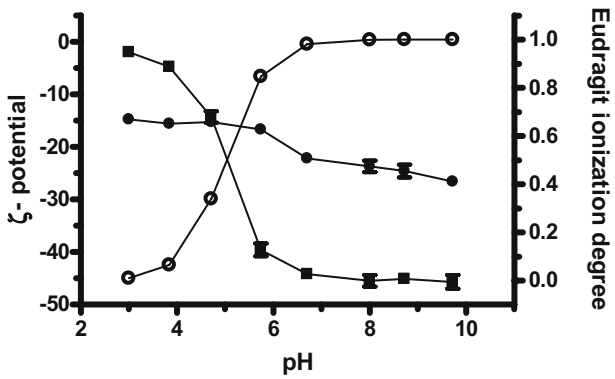

Fig. 2. ζ-potential (*y-axis left*) variation of nanoparticles MA7 (*filled square*) and SA7 (*filled circle*), and Eudragit (*open circle*) ionization degree (*y-axis right*) as a function of pH variation. Results are the mean of three independent experiments (± SD).

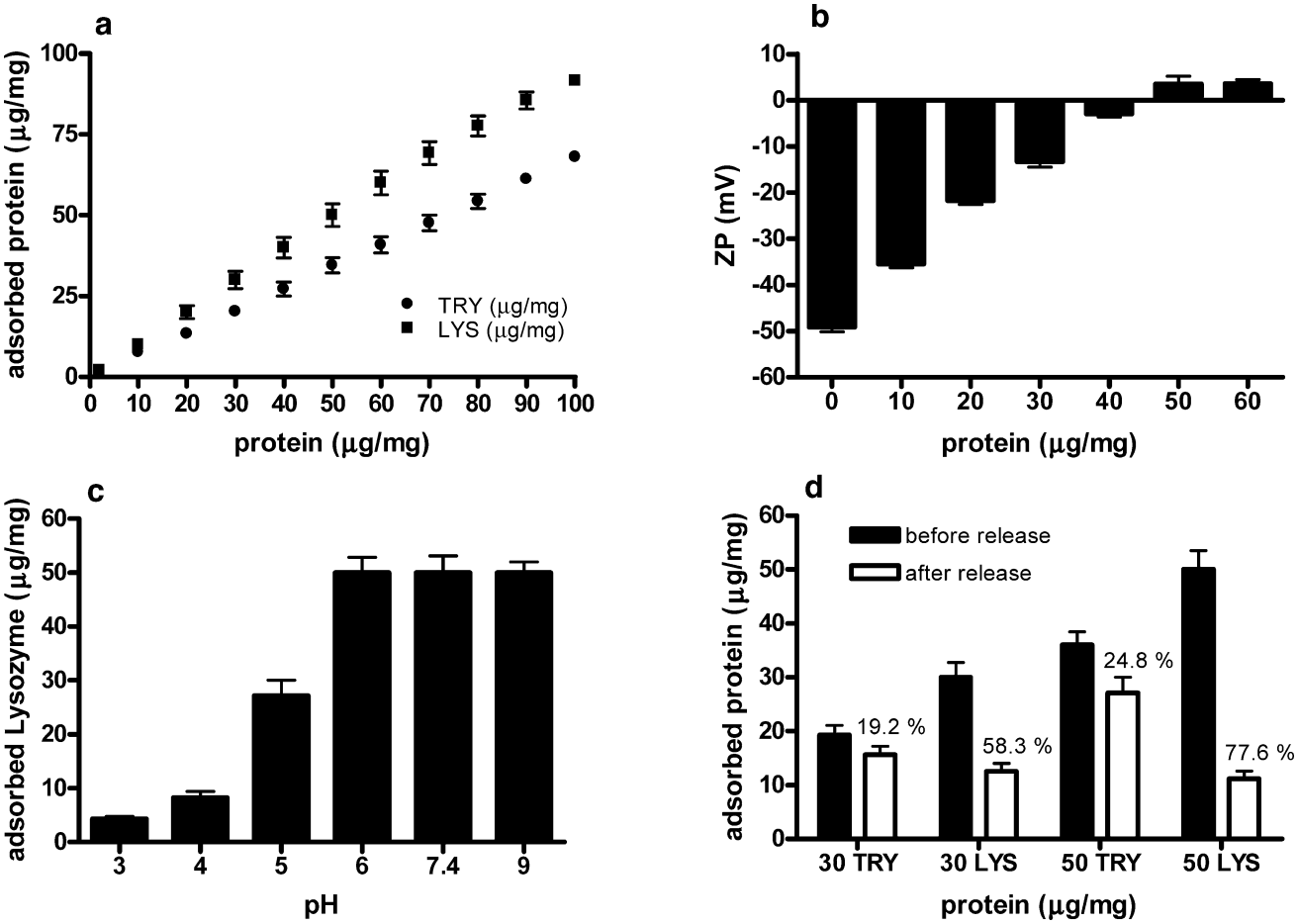

Fig. 3. Binding and release properties of carboxylated core-shell MA7 nanoparticles. **a** Protein adsorption. MA7 nanoparticles (5 mg/ml) were incubated with increasing amounts of Lysozyme or Trypsin proteins (10–500 µg/ml) in 1 ml of 20 mM phosphate buffer (pH 7.4). The adsorption efficiency and the loading values were calculated from the difference between the fed and the unbound protein as described in the "MATERIALS AND METHODS" section. Results are the mean of three independent experiments (± SD). **b** ζ-potential variation upon Lysozyme adsorption (0–300 µg/ml) on MA7 nanoparticles in water (10 mM NaCl) pH 6.5. Results are the mean of three independent experiments (± SD). **c** Lysozyme adsorption on MA7 nanoparticles as a function of pH in the range 3–9. Results are the mean of three independent experiments (± SD). **d** Protein release from MA7 nanoparticles. MA7/protein complexes with different loading values (obtained from 150 and 250 µg protein/5 mg MA7/1 ml) were washed twice with phosphate buffer and resuspended in 1 ml of 20 mM phosphate buffer (pH 7.4) added with 1 M NaCl for 30 min at 37°C. The release efficiency and the amount of released protein were calculated as described in the "MATERIALS AND METHODS" section. Results are the mean of three independent experiments (± SD).

tein, being much more efficient with Lysozyme, the protein with lower molecular weight and higher isoelectric point.

Protein adsorption on the outer surface of these nanoparticles was also confirmed by means of dynamic light scattering tecniques. Following addition of increasing amounts of Lysozyme (0–300 µg/ml) and removal of unbound protein, a progressive increase in both ζ-potential values (Fig. 3b) and hydrodynamic diameters (from 237.8 to 328 nm) of MA7/protein complexes was observed.

To elucidate the mechanism of interaction, the same binding experiments were run in the presence of buffers with different salt or pH concentration. Lysozyme and Trypsin adsorption efficiency was very high in 20 mM phosphate buffer (pH 7.4), whereas it was gradually reduced in the presence of higher salt concentration, and it was strongly inhibited in 1 M NaCl (data not shown), thus indicating that ionic interaction may be the major driving force in protein/nanoparticle complex formation. Finally, MA7 binding ability was the same in the pH range 6–10, but it was seriously affected by pH decrease especially in the presence of higher protein concentration (Fig. 3c), mainly due to suspension destabilization following Eudragit protonation.

To assess the reversibility of the interaction, desorption experiments were run at 37°C in 20 mM phosphate buffer (pH 7.4) added with 1 M NaCl (Fig. 3d). The results showed that Lysozyme release was generally more extensive than Trypsin release, being 58 and 19%, respectively, when complexes were prepared with 150 µg protein/5 mg particles/1 ml. In addition, for both proteins, release efficiency was more extensive from complexes with higher loading values. For example, when complexes with 50 µg/mg of bound Lysozyme were employed (5% w/w), the release efficiency increased up to 78%. Protein desorption in high strenght ionic buffers shows that the interaction is reversible and suggests that protein release could be modulated according to the starting loading values and the intrinsic protein properties.

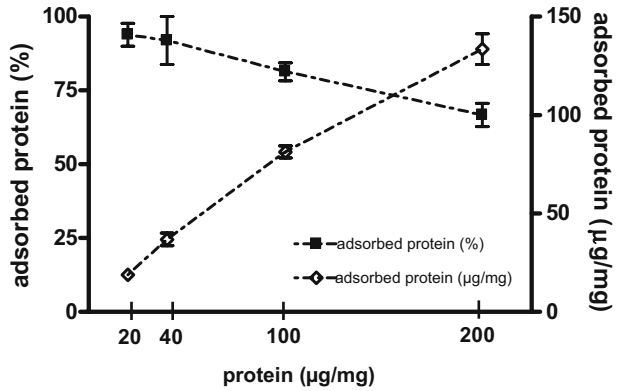

Fig. 4. MA7 core-shell nanoparticles bind HIV-1 Tat protein. Nanoparticles were resuspended at 1 mg/ml and incubated (50 µl) with increasing amounts (1, 2, 5 and 10 µg) of HIV-1 Tat protein. Bound protein was removed from the complexes, analysed by SDS-polyacrylamide gel electrophoresis and quantified with the GelDoc Quantity One System, as described in the "MATERIALS AND METHODS" section. Data are the mean of three independent experiments (± SEM).

MA7 Nanoparticles Adsorb HIV-1 Tat Protein

In view of their possible application as delivery system for vaccine development, the capability of the MA7 nanoparticles to bind a relevant vaccine antigen was also tested using the HIV-1 Tat protein, which is a basic protein due to the presence of a positively charged region in its sequence, rich in argine and lysine. However, due to the high production costs of biologically active GLP-grade Tat, these sets of experiments were carried out using smaller volumes and a different method to detect the unbound protein. To this goal, complexes were prepared with increasing doses (1–10 µg) of Tat and an equal amount (50 µl) of MA7 nanoparticles previously resuspended in PBS at 1 mg/ml (corresponding to 20–200 µg/mg of particles/ml). Tat bound to the nanoparticles surface was then removed from the complexes, analyzed by SDS-PAGE electrophoresis and quantified. The results, shown in Fig. 4, indicated that Tat adsorbs with high efficiency and in a reproducible dose-dependent manner at the surface of the MA7 nanoparticles. Maximum binding was detected at 20–40 µg of Tat/mg MA7/ml with loading values of 19–37 µg/mg, i.e. 1.9–3.7 w/w. Although slightly decreased, a very efficient binding of approximately 80 and 65% was detected at 100 and 200 µg of Tat/mg MA7/ml, respectively, with loading values of 80 and 130 µg/mg, i.e. 8–13% w/w. These results are similar to those obtained with Trypsin and Lysozyme when the same protein/nanoparticles w/w ratios are employed.

Analysis of *in Vitro* Cytotoxicity

The cytotoxicity of sample MA7 was assayed in HL3T1 and in monocyte-derived dendritic cells following incubation with increasing amounts of nanoparticles (10–500 µg/ml) alone or associated with Tat (1 µg). As shown in Fig. 5, no reduction in cell viability was observed up to 500 µg/ml of MA7 alone or associated with Tat as compared to untreated cells ($p > 0.05$) or to cells treated with free Tat ($p > 0.05$). These data indicate that the MA7 nanoparticles are not toxic for the cells. Based on the results, the dose of 30 µg/ml was selected for further studies in cellular systems.

Cellular Uptake of MA7/Protein Complexes and Analysis of Functional Protein Release

For their application as delivery systems in vaccine development, polymeric nanoparticles should bind, deliver and release the protein in its biologically active conformation. This is particularly important for proteins requiring native conformation for vaccine efficacy, such as the HIV-1 Tat (31–33). Therefore, the capability of the MA7 nanoparticles to bind, deliver and release the HIV-1 Tat protein in its biologically active conformation was determined in HL3T1 cells, containing an integrated copy of the bacterial chloramphenicol acetyl transferase (CAT) reporter gene under the HIV-1 LTR promoter. In these cells expression of the CAT gene occurs only in the presence of biologically active HIV-1 Tat protein which is essential for trans-activation of the HIV-1 LTR promoter. Cells were incubated

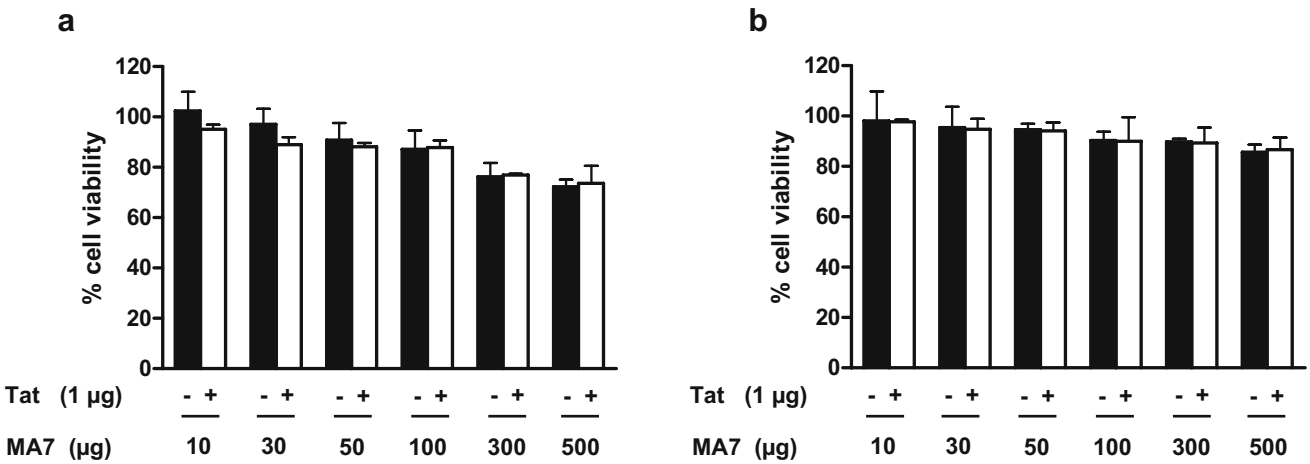

Fig. 5. Analysis of *in vitro* cytotoxicity. HL3T1 cells (**a**) and MDDC (**b**) were cultured for 96 h with increasing doses of MA7 alone (*black bars*) or complexed with Tat (*white bars*). Controls were represented by untreated cells or cells cultured with Tat alone. The percentage (%) of cell viability as compared to control cells was determined as described in the "MATERIALS AND METHODS" section, and the results represent the mean of three independent experiments (± SEM).

with freshly prepared complexes, composed of increasing doses (0.125, 0.5, 1 μg/ml) of biologically active Tat bound to the MA7 nanoparticles (30 μg/ml), or with Tat alone, and CAT activity was evaluated 48 h later. As shown in Fig. 6a, expression of CAT was maximal and similar in cells treated with fresh MA7/Tat nanoparticle complexes and in cells incubated with the same dose of Tat alone ($p > 0.05$). These results indicate that the MA7 nanoparticles bind, deliver and allow intracellular release of a bioactive protein from the complex.

MA7 Nanoparticles Protect Tat From Oxidation

A peculiar feature of the HIV-1 Tat protein is that it oxidizes very easily with air and light and is labile at room temperature due to the presence of seven cysteines in its sequence. Oxidation leads to protein multimerization, aggregation and loss of the biological activity which requires a native momeric protein conformation (20,21). Therefore, special procedures must be followed for purification, handling and storage of recombinant Tat in order to preserve its native conformation. Of note, a fully biologically active Tat protein is required for the immunomodulatory effects of Tat and for control of replication and block of disease progression in monkeys vaccinated with Tat and challenged with a pathogenic simian immunodeficiency virus (21,34–36). Thus, to determine whether Tat bound to the nanoparticles was protected from oxidation, MA7/Tat protein complexes or Tat alone were insufflated with air and exposed to light for 24 h at room temperature before the addition to the HL3T1 cells. As shown in Fig. 6b, when Tat was previously adsorbed onto the nanoparticles surface, the exposure to air and light did not inactivate Tat trans-activating function, whereas when Tat was free it caused oxidation and a significant loss of Tat biological activity ($p < 0.001$). Thereby, Tat bound to the nanoparticles was protected from oxidation.

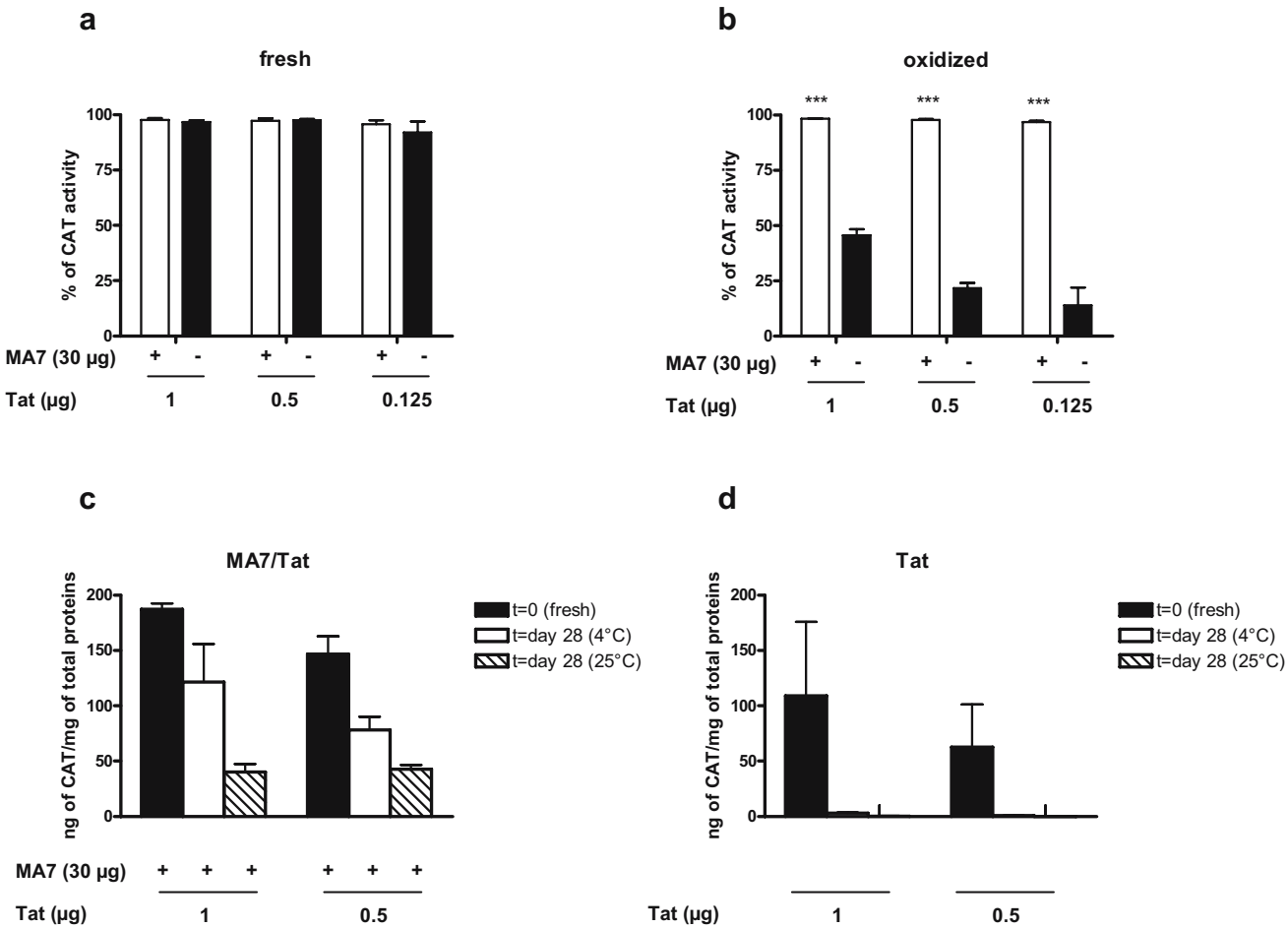

Fig. 6. Polymeric MA7 core-shell nanoparticles deliver, release and increase the stability of a biologically active HIV-1 Tat protein. HL3T1 cells were incubated with increasing amounts of Tat (0.125, 0.5 and 1 μg/ml) bound to MA7 nanoparticles (30 μg/ml) or with the same amount of Tat alone. Samples were added to cells immediately (**a**) or after oxidation treatment (**b**). After 48 h, the percentage of CAT activity was calculated as described in the "MATERIALS AND METHODS" section. Results in **a** are the mean of five independent experiments (± SEM). Results in **b** are the mean of three independent experiments (± SEM). *Three asterisks* indicate significant difference of CAT activity between the MA7/Tat complexes and Tat alone with $p < 0.001$. In **c** and **d**, HL3T1 cells were incubated with 0.5 or 1 μg/ml of HIV-1 Tat bound to MA7 nanoparticles (30 μg/ml) (**c**) or with the same dose of Tat alone (**d**). Samples were added to the cells immediately ($t = 0$) or after storage for 4 weeks ($t =$ day 28) at 4 and 25°C. After 48 h, the amount of CAT expression (ng/mg) was calculated as described in the "MATERIALS AND METHODS" section. The results in **c** and **d** are the mean of three independent experiments (± SEM).

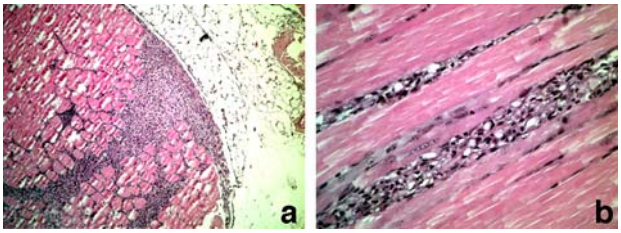

Fig. 7. Histological examination of murine tissues after two injections of MA7/Tat complexes or MA7 nanoparticles alone by the i.m. route. One representative mouse is shown. A dense and diffuse infiltration of inflammatory cells is shown around the muscular cells (**a**), and in the endomysium connective tissue (**b**). Infiltrative inflammatory cells are predominantly macrophages. Hematoxilyn–Eosin staining: **a** 50X; **b** 400X. No local alterations were observed in mice inoculated i.n. No alterations that may be related to injection of MA7 were reported in the other organs examined (kidney, heart, lungs, intestine, liver, brain, spleen and draining lymph nodes).

Finally, to evaluate the stability of the formulation, MA7/Tat complexes were prepared using 30 μg of nanoparticles and increasing doses of Tat (0.5–1 μg). Complexes were added immediately to the cells, or stored for 28 days at 4 and 25°C and then added to the cells. As shown in Fig. 6c, adsorption of Tat to the nanoparticles significantly preserved Tat biological activity up to 28 days at 4°C, whereas incubation of free Tat for 28 days in aqueous solution at 4°C caused a dramatic loss of Tat activity (Fig. 6d). Interestingly, when complexes were stored for 28 days at 25°C, Tat activity was still preserved although at lower extent (Fig. 6c), whereas incubation of free Tat for 28 days in aqueous solution at 25°C caused the complete loss of Tat activity (Fig. 6d).

As a whole, these results indicate that adsorption of Tat to the nanoparticles surface preserves the native conformation of the protein and protects it from oxidation thus increasing its stability and shelf-life. The most likely explanation of this effect is that the highly hydrophilic outer shell accommodates Tat molecules (monomers) in the Eudragit chains composing the shell. This may likely prevent protein multimerization and loss of biological activity before its addition to the cells thus maintaining Tat active conformation. This is also in agreement with previous results obtained with similar microparticles composed of PMMA and Eudragit (26,37).

Mice Studies

An important concern in the development of new delivery systems/adjuvants is their safety and lack of toxicity *in vivo*. Thus, groups of mice were inoculated with MA7 alone or with MA7/Tat either i.m. at weeks 0 and 4, or i.n. at days 0, 7, 14 and 21. The site of injection and the general health of the mice were monitored twice a week and no signs of local or systemic adverse reactions were ever observed. In general, in all mice no specific alterations that may be related to injection of the nanoparticles were reported in the organs examined (kidney, heart, lungs, intestine, liver, brain, spleen

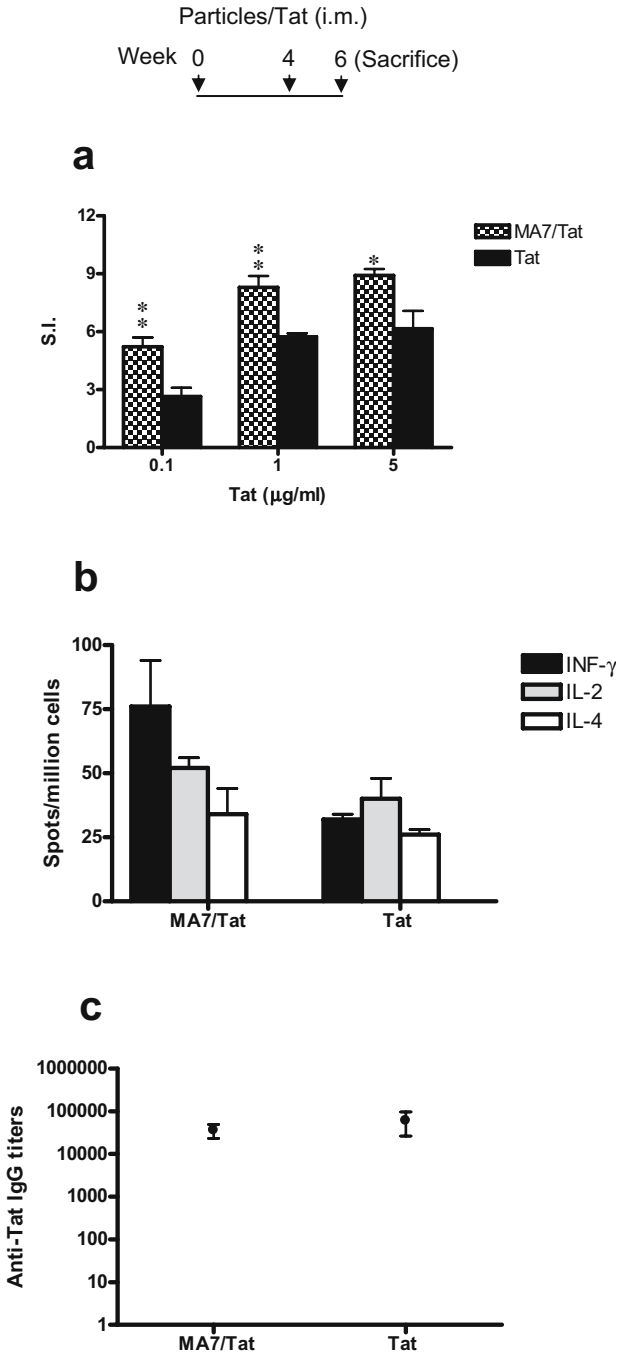

Fig. 8. Analysis of Tat-specific immune responses after i.m. immunization with MA7/Tat or Tat alone. Mice were immunized at week 0 and 4 and sacrificed 15 days after the last immunization. **a** Lymphoproliferation to Tat protein. Values represent the S.I. of murine splenocytes (pool of spleens) after Tat (0.1, 1 or 5 μg/ml) addition. The results of one representative experiment are shown. *Double asterisks*, $p < 0.01$; *Single asterisk*, $p < 0.05$. **b** Analysis of Tat-induced INF-γ, IL-2 and IL-4 secretion by Elispot. Spleens were pooled for each experimental group, added to Elispot plates pre-coated with the cytokine-specific capture antibody, and incubated in the absence (untreated) or presence of the VCF peptide. Specific responses corresponded to the number of spots counted in the peptide-treated wells minus the number of spots counted in the untreated wells. Responses were considered significant when net spots/million cells were ≥30 and at least two-fold above the score of the untreated wells. The results of one representative experiment are shown. **c** Anti-Tat IgG titers. Antibody titers were measured by ELISA. Results are expressed as the reciprocal log of the arithmetic mean endpoint titers (± SEM) of mice sera tested individually.

and draining lymph nodes). In mice ($n = 15$) receiving i.n. inoculations, no local alterations were observed, whereas in mice inoculated i.m., infiltrations of inflammatory cells were observed in 7/11 mice treated with MA7/Tat (63%) and in 4/5 animals inoculated with MA7 alone (80%) at the site of injection. As shown in Fig. 7, histological examination of these lesions showed irregular widening of endomysial connective septa owing to a dense and diffuse infiltration of inflammatory cells surrounding the muscular cells. Infiltrative inflammatory cells were predominantly macrophages with large and vacuolated cytoplasm and central nuclei. Adjacent muscular cells were characterized by regressive changes. Although preliminary, these results suggest that the MA7 nanoparticles are well tolerated *in vivo* and deserve further characterization for vaccination purposes.

Thereby, groups of mice ($n = 5$) were immunized with MA7/Tat, Tat alone or the naked nanoparticles at weeks 0 and 4 by the i.m. route and sacrificed 15 days after the last immunization. As the delivery of a protein antigen by means of a particulate vectors may increase of cellular responses to the antigen (38), cell proliferation in response to the Tat protein was evaluated using the [^{3}H]-Thymidine incorporation test on mice splenocytes cultured for 5 days in the presence of 0.1, 1 and 5 μg/ml of Tat. Antigen-specific and dose-dependent cell proliferation was detected in both groups of mice immunized with MA7/Tat and Tat alone (Fig. 8a), but not in the untreated splenocytes nor in lymphocytes of control mice injected with MA7 alone. The proliferation index was significantly higher in mice immunized with MA7/Tat, as compared to mice vaccinated with Tat ($p < 0.01$ for the 0.1 and 1 μg doses and $p < 0.05$ for the 5 μg dose).

To evaluate the nature of the cytokine profile generated by vaccination, splenocytes were also tested using the Elispot technique to evaluate production of Th1-type (INFγ and IL-2) and Th2-type (IL-4) responses. The results indicated that INFγ and IL-2 responses were higher in mice vaccinated with the MA7/Tat vaccine formulation as compared to immunization with Tat alone, although the differences in this assay were not statistically significant ($p > 0.05$). In contrast, IL-4 responses were low and comparable in both groups (Fig. 8b). Finally, the analysis of antigen-specific IgG titers showed that immunization with the MA7/Tat formulation elicited significant antibody titers in a fashion similar to immunization with the Tat protein alone (Fig. 8c).

As a whole the results indicate that the presence of the nanoparticles in the vaccine formulation increases the antigen-specific cellular responses, with a prevalence of Th1-type responses, and promotes an efficient priming of humoral responses.

DISCUSSION

Several previous studies described the improvement of vaccines by antigen encapsulation into liposomes (39) and biodegradable polymers (18). However, it has been well-established that the encapsulation and release processes expose the antigen to a variety of damaging conditions that often lead to instability and degradation (8,40). The surface adsorption strategy avoids problems of protein instability and/or incomplete release following antigen encapsulation in biodegradable microparticles and seems to be very efficient to induce broad and potent immune responses, as recently shown by studies describing the use of anionic PLG microparticles, polymeric lamellar substrate particles and anionic wax nanoparticles for protein adsorption (12,41,42). However, most of these systems require the addition of surfactants which may cause low reproducibility and instability of the vaccine formulations thus limiting their use in humans (14,40).

Among the surfactant free systems, the core-shell nanoparticles here described show some novel and distinguishing features. The MA7 nanoparticles are obtained by a fine controlled polymerization of the single acrylic monomers in water and not by surface functionalization or chemical conjugation of charged polymers to the preformed particles (14,28,30,43). Our synthetic procedure consists of a single step particle forming method involving an emulsion-type polymerization in which the conventional emulsifier agent is substituted with a polymeric electro-steric stabilizer. In these conditions, both the particle size and their surface functionality are dictated by the nature of the polymeric stabilizer thus leading to great opportunities to prepare specifically designed particles. In particular, since the particles surface can be tailored with positively and negatively charged groups (15,26,37,44–46), the advantage of this delivery system is that ionic interactions with proteins characterized by different isoelectric points can be envisaged. In addition, the synthetic procedure of the MA7 nanoparticles does not require the use of organic solvents, which may impair clinical development, and allows the large scale preparation of very homogeneous and reproducible samples and, hence, the feasibility of scaling-up for future clinical development. Of note, the nanoparticles described in the present study are very stable in aqueous suspension and in powder form for at least 36 months. Finally, their protein formulations are very easy and fast to be prepared since they spontaneously assemble in aqueous solution following incubation of the two components for 1 h and no purification steps are required.

The results of this study show that these core-shell nanoparticles efficiently and reversibly adsorb high amounts of basic proteins (up to 20% w/w) differing in size and isoelectric point, with greater loading ability if compared to other colloidal systems described in the literature (14,28,30,47). Protein adsorption occurs rapidly, is highly reproducible and mainly driven by ionic interaction as it is inhibited by high ionic strength buffers and low pH. Binding is reversible since extensive desorption occurs in the presence of high salt concentration. Also, MA7 nanoparticles reversibly bind with high efficiency a vaccine relevant antigen such as HIV-1 Tat on their surface with loading up to about 13% w/w in the protein concentration range tested. Noteworthy, the results in cell-free and in tissue culture systems demonstrate that they bind Tat in its bioactive conformation, that Tat is released as bioactive protein into the cells, and that they increase the stability and shelf-life of the protein in aqueous solution up to 4 weeks.

In addition, these nanoparticles are not cytotoxic *in vitro,* and are well-tolerated *in vivo,* both after i.m and i.n. inoculation, in agreement with the results of previous studies in mice and in monkeys with microparticles of 2–7 μm in diameter and similar PMMA-Eudragit composition (26)

(Caputo *et al.*, unpublished results). Further toxicological and biodistribution studies are certainly needed before clinical testing of these nanoparticles. However, it is noteworthy that the preparation of these nanoparticles foresees the employment of biocompatible and pharmaceutically acceptable excipients such as PMMA, already shown to be slowly degradable in the form of nanoparticles (48–50), and Eudragit L100-55, already approved for oral use in humans (http://www.roehm.de/en/pharmapolymers.html). Based on the knowledge reported in the literature regarding PMMA toxicology and biodistribution (50–54), and considering that vaccine approaches require a very limited number of immunization/boost steps in a life-time not by the intravenous route, and hence inoculation of very low doses of nanoparticles, the risk deriving from polymer accumulation seems to be very low. In addition, while controlled biodegradation of the delivering polymer is necessary when the antigen is encapsulated and/or entrapped in the polymeric matrix, it might not be an essential requirement when the antigen is adsorbed on the surface and only few shots are envisaged in a life-time, which is a desirable requirement for vaccines especially against infectious disease agents.

Tat is very labile to air, light and temperature and several precautions are needed for the handling and storage of Tat to avoid oxidation and loss of biological activity. However, the demonstration that these novel polymeric nanoparticles protect a bioactive protein from oxidation is an interesting feature for their application as vaccine delivery systems, in particular for development of vaccines for which immunization with the bioactive form of the antigen is an important requirement, and for vaccines to be delivered in countries where refrigeration and safe storage conditions are not easily available. Previous studies have shown that bioactive Tat, but not oxidized Tat, is efficiently taken up by DC at picomolar concentrations, induces their maturation and increases their antigen presentation capability, functioning as both antigen and adjuvant toward Th-1 type immune responses (21,34). Vaccination with native Tat or *tat* DNA controlled replication and blocked disease progression in vaccinated monkeys challenged with the highly pathogenic simian-human immunodeficiency virus (34,35). Other studies have shown that immunisation with a synthetic Tat protein (Tat Oyi) elicited protective anti-Tat antibodies in the macaque SHIV model of infection, whereas in rabbits it induced cross-clade anti-Tat antibodies (55). In other settings, Tat vaccines did not provide significant protective immunity and escape mutants have been observed (56–58). However whether these apparently conflicting results are due to the nature of the vaccine antigen (DNA, protein, native or inactivated Tat protein), the monkey species, the route of the administration, the antigen dose and schedule of immunization, the adjuvant used, or the virus challenge dose, still remains to be elucidated (59).

In addition, recent evidence also indicates that the biologically active Tat protein displays immunomodulatory activities which can be exploited for the development of a combined subunits vaccine (33,60–62) (Gavioli *et al.*, unpublished results). Thus, the present results imply that the combination of slow release and depot effect of the nanoparticles complexes, together with the preservation of the biological active conformation, may reduce the amount of antigen used in the vaccine and reduce the number of booster shots necessary for the success of vaccination. In addition, the handling, storage and shelf-life of such vaccine formulations may be greatly simplified. Finally, the presented results indicate that these nanoparticles increase the cellular immunogenicity of the antigen after i.m. administration in mice and induce significant antigen-specific humoral responses. As a whole, these results indicate that this delivery system deserves further characterization for vaccine applications.

CONCLUSIONS

Controlled emulsion polymerization of methylmethacrylate in the presence of commercial Eudragit L100-55 leads to the formation of reproducible core-shell nanoparticles, with high surface charge density deriving from the carboxyl groups located in the hydrophilic shell. These nanoparticles are able to specifically and reversibly adsorb on their surface large amounts (up to 20% w/w in the described experimental conditions) of model basic proteins (Lysozyme, Trypsin) and of a relevant vaccine antigen (HIV-1 Tat), mainly through ionic interactions, and to release them extensively. The nanoparticles are not toxic *in vitro,* and are well tolerated in mice after intramuscular or intranasal administration. In addition, they efficiently deliver and release HIV-1 Tat intracellularly, protect it from oxidation and preserve its biological activity, increasing its shelf-life which is particularly noteworthy for vaccine applications especially in developing countries. Finally, the results indicate that these nanoparticles increase the cellular immunogenicity of the antigen after i.m. administration in mice and induce significant antigen-specific humoral responses. This technology ensures the large scale preparation of safe surfactant free nanoparticles, and it greatly simplifies the storage and handling of vaccine formulations. Thus, the described core-shell nanoparticles represent a promising delivery system for parenteral and mucosal vaccination with protein subunit vaccines, particularly when a native protein conformation is required.

ACKNOWLEDGEMENTS

This work was supported by grants from the Istituto Superiore di Sanità [Italian Concerted Action on HIV-AIDS Vaccine Development (ICAV)], and from the Ministero dell'Istruzione, dell'Università e della Ricerca (MIUR). We are grateful to Mauro Magnani (Diatheva, Fano, Italy) for providing batches of HIV-1 Tat protein and to Marina Tomelli for experimental assistance.

REFERENCES

1. W. M. Kast, R. Offringa, P. J. Peters, A. C. Voordouw, R. H. Meloen, A. J. van der Eb, and C. J. Melief. Eradication of adenovirus E1-induced tumors by E1A-specific cytotoxic T lymphocytes. *Cell* **59**:603–614 (1989).
2. H. L. Hanson, D. L. Donermeyer, H. Ikeda, J. M. White, V. Shankaran, L. J. Old, H. Shiku, R. D. Schreiber, and P. M. Allen. Eradication of established tumors by CD8+ T cell adoptive immunotherapy. *Immunity* **13**:265–276 (2000).
3. M. A. Brehm, L. K. Selin, and R. M. Welsh. CD8 T cell responses to viral infections in sequence. *Cell Microbiol.* **6**:411–421 (2004).

4. J. A. Berzofsky, J. D. Ahlers, J. Janik, J. Morris, S. Oh, M. Terabe, and I. M. Belyakov. Progress on new vaccine strategies against chronic viral infections. *J. Clin. Invest.* **114**:450–462 (2004).
5. J. A. Berzofsky, M. Terabe, S. Oh, I. M. Belyakov, J. D. Ahlers, J. E. Janik, and J. C. Morris. Progress on new vaccine strategies for the immunotherapy and prevention of cancer. *J. Clin. Invest.* **113**:1515–1525 (2004).
6. M. M. Levine, and M. B. Sztein. Vaccine development strategies for improving immunization: The role of modern immunology. *Nat. Immunol.* **5**:460–464 (2004).
7. M. van de Weert, W. E. Hennink, and W. Jiskoot. Protein instability in poly(lactic-co-glycolic acid) microparticles. *Pharm. Res.* **17**:1159–1167 (2000).
8. H. Tamber, P. Johansen, H. P. Merkle, and B. Gander. Formulation aspects of biodegradable polymeric microspheres for antigen delivery. *Adv. Drug. Deliv. Rev.* **57**:357–376 (2005).
9. D. T. O'Hagan. Recent developments in vaccine delivery systems. *Curr Drug Targets Infect Disord* **1**:273–286 (2001).
10. D. T. O'Hagan, and E. Lavelle. Novel adjuvants and delivery systems for HIV vaccines. *Aids* **16**(4):S115–S124 (2002).
11. D. T. O'Hagan, and M. Singh. Microparticles as vaccine adjuvants and delivery systems. *Expert Rev. Vaccines* **2**:269–283 (2003).
12. D. T. O'Hagan, M. Singh, and J. B. Ulmer. Microparticles for the delivery of DNA vaccines. *Immunol. Rev.* **199**:191–200 (2004).
13. D. Sesardic, and R. Dobbelaer. European union regulatory developments for new vaccine adjuvants and delivery systems. *Vaccine* **22**:2452–2456 (2004).
14. Y. Ataman-Onal, S. Munier, A. Ganee, C. Terrat, P. Y. Durand, N. Battail, F. Martinon, R. Le Grand, M. H. Charles, T. Delair, and B. Verrier. Surfactant-free anionic PLA nanoparticles coated with HIV-1 p24 protein induced enhanced cellular and humoral immune responses in various animal models. *J. Control. Release* **112**:175–185 (2006).
15. B. Ensoli, A. Caputo, M. Laus, L. Tondelli, and K. Sparnacci. Nanoparticles for delivery of a pharmacologically active agent, UK, PCT/EP2004/012420, WO2005/048997.
16. Z. Cui, J. Patel, M. Tuzova, P. Ray, R. Phillips, J. G. Woodward, A. Nath, and R. J. Mumper. Strong T cell type-1 immune responses to HIV-1 Tat (1–72) protein-coated nanoparticles. *Vaccine* **22**:2631–2640 (2004).
17. J. Patel, D. Galey, J. Jones, P. Ray, J. G. Woodward, A. Nath, and R. J. Mumper. HIV-1 Tat-coated nanoparticles result in enhanced humoral immune responses and neutralizing antibodies compared to alum adjuvant. *Vaccine* **24**:3564–3573 (2006).
18. M. Singh, J. Kazzaz, M. Ugozzoli, P. Malyala, J. Chesko, and D. T. O'Hagan. Polylactide-co-glycolide microparticles with surface adsorbed antigens as vaccine delivery systems. *Curr. Drug Deliv.* **3**:115–120 (2006).
19. B. Ensoli, L. Buonaguro, G. Barillari, V. Fiorelli, R. Gendelman, R. A. Morgan, P. Wingfield, and R. C. Gallo. Release, uptake, and effects of extracellular human immunodeficiency virus type 1 Tat protein on cell growth and viral transactivation. *J. Virol.* **67**:277–287 (1993).
20. B. Ensoli, V. Fiorelli, F. Ensoli, A. Cafaro, F. Titti, S. Butto, P. Monini, M. Magnani, A. Caputo, and E. Garaci. Candidate HIV-1 Tat vaccine development: From basic science to clinical trials. *Aids* **20**:2245–2261 (2006).
21. E. Fanales-Belasio, S. Moretti, F. Nappi, G. Barillari, F. Micheletti, A. Cafaro, and B. Ensoli. Native HIV-1 Tat protein targets monocyte-derived dendritic cells and enhances their maturation, function, and antigen-specific T cell responses. *J. Immunol.* **168**:197–206 (2002).
22. A. Castaldello, E. Brocca-Cofano, R. Voltan, C. Triulzi, G. Altavilla, M. Laus, K. Sparnacci, M. Ballestri, L. Tondelli, C. Fortini, R. Gavioli, B. Ensoli, and A. Caputo. DNA prime and protein boost immunization with innovative polymeric cationic core-shell nanoparticles elicits broad immune responses and strongly enhance cellular responses of HIV-1 tat DNA vaccination. *Vaccine* **24**:5655–5669 (2006).
23. P. K. Smith. Measurement of protein using bicinchoninic acid. *Analytical Biochemistry* **150**:76–85 (1985).
24. M. Betti, R. Voltan, M. Marchisio, I. Mantovani, C. Boarini, F. Nappi, B. Ensoli, and A. Caputo. Characterization of HIV-1 Tat proteins mutated in the transactivation domain for prophylactic and therapeutic application. *Vaccine* **19**:3408–3419 (2001).
25. A. Caputo, R. Gavioli, G. Altavilla, E. Brocca-Cofano, C. Boarini, M. Betti, A. Castaldello, F. Lorenzini, F. Micheletti, A. Cafaro, K. Sparnacci, M. Laus, L. Tondelli, and B. Ensoli. Immunization with low doses of HIV-1 tat DNA delivered by novel cationic block copolymers induces CTL responses against Tat. *Vaccine* **21**:1103–1111 (2003).
26. A. Caputo, E. Brocca-Cofano, A. Castaldello, R. De Michele, G. Altavilla, M. Marchisio, R. Gavioli, U. Rolen, L. Chiarantini, A. Cerasi, S. Dominici, M. Magnani, A. Cafaro, K. Sparnacci, M. Laus, L. Tondelli, and B. Ensoli. Novel biocompatible anionic polymeric microspheres for the delivery of the HIV-1 Tat protein for vaccine application. *Vaccine* **22**:2910–2924 (2004).
27. E. Caselli, M. Betti, M. P. Grossi, P. G. Balboni, C. Rossi, C. Boarini, A. Cafaro, G. Barbanti-Brodano, B. Ensoli, and A. Caputo. DNA immunization with HIV-1 tat mutated in the trans activation domain induces humoral and cellular immune responses against wild-type Tat. *J. Immunol.* **162**: 5631–5638 (1999).
28. T. Jung, W. Kamm, A. Breitenbach, K. D. Hungerer, E. Hundt, and T. Kissel. Tetanus toxoid loaded nanoparticles from sulfobutylated poly(vinyl alcohol)-graft-poly(lactide-co-glycolide): Evaluation of antibody response after oral and nasal application in mice. *Pharm. Res.* **18**:352–360 (2001).
29. B. Mandal, M. Kempf, H. P. Merkle, and E. Walter. Immobilisation of GM-CSF onto particulate vaccine carrier systems. *Int. J. Pharm.* **269**:259–265 (2004).
30. T. Akagi, T. Kaneko, T. Kida, and M. Akashi. Preparation and characterization of biodegradable nanoparticles based on poly (gamma-glutamic acid) with l-phenylalanine as a protein carrier. *J. Control Release* **108**:226–236 (2005).
31. A. Caputo, R. Gavioli, and B. Ensoli. Recent advances in the development of HIV-1 Tat-based vaccines. *Curr. HIV Res.* **2**:357–376 (2004).
32. F. Ferrantelli, A. Cafaro, and B. Ensoli. Nonstructural HIV proteins as targets for prophylactic or therapeutic vaccines. *Curr. Opin. Biotechnol.* **15**:543–556 (2004).
33. B. Ensoli, A. Cafaro, A. Caputo, V. Fiorelli, F. Ensoli, R. Gavioli, F. Ferrantelli, A. Cara, F. Titti, and M. Magnani. Vaccines based on the native HIV Tat protein and on the combination of Tat and the structural HIV protein variant DeltaV2 Env. *Microbes Infect.* **7**:1392–1399 (2005).
34. A. Cafaro, A. Caputo, C. Fracasso, M. T. Maggiorella, D. Goletti, S. Baroncelli, M. Pace, L. Sernicola, M. L. Koanga–Mogtomo, M. Betti, A. Borsetti, R. Belli, L. Akerblom, F. Corrias, S. Butto, J. Heeney, P. Verani, F. Titti, and B. Ensoli. Control of SHIV-89.6P-infection of cynomolgus monkeys by HIV-1 Tat protein vaccine. *Nat. Med.* **5**:643–650 (1999).
35. A. Cafaro, F. Titti, C. Fracasso, M. T. Maggiorella, S. Baroncelli, A. Caputo, D. Goletti, A. Borsetti, M. Pace, E. Fanales-Belasio, B. Ridolfi, D. R. Negri, L. Sernicola, R. Belli, F. Corrias, I. Macchia, P. Leone, Z. Michelini, P. ten Haaft, S. Butto, P. Verani, and B. Ensoli. Vaccination with DNA containing tat coding sequences and unmethylated CpG motifs protects cynomolgus monkeys upon infection with simian/human immunodeficiency virus (SHIV89.6P). *Vaccine* **19**:2862–2877 (2001).
36. M. T. Maggiorella, S. Baroncelli, Z. Michelini, E. Fanales-Belasio, S. Moretti, L. Sernicola, A. Cara, D. R. Negri, S. Butto, V. Fiorelli, A. Tripiciano, A. Scoglio, A. Caputo, A. Borsetti, B. Ridolfi, R. Bona, P. ten Haaft, I. Macchia, P. Leone, M. R. Pavone-Cossut, F. Nappi, M. Ciccozzi, J. Heeney, F. Titti, A. Cafaro, and B. Ensoli. Long-term protection against SHIV89.6P replication in HIV-1 Tat vaccinated cynomolgus monkeys. *Vaccine* **22**:3258–3269 (2004).
37. K. Sparnacci, M. Laus, L. Tondelli, C. Bernardi, L. Magnani, F. Corticelli, M. Marchisio, B. Ensoli, A. Castaldello, and A. Caputo. Core-shell microspheres by dispersion polymerization as promising delivery systems for proteins. *J. Biomater. Sci. Polym. Ed.* **16**:1557–1574 (2005).
38. T. Storni, T. M. Kundig, G. Senti, and P. Johansen. Immunity in response to particulate antigen-delivery systems. *Adv. Drug Deliv. Rev.* **57**:333–355 (2005).
39. D. Felnerova, J. F. Viret, R. Gluck, and C. Moser. Liposomes

and virosomes as delivery systems for antigens, nucleic acids and drugs. *Curr. Opin. Biotechnol.* **15**:518–529 (2004).
40. W. Jiang, R. K. Gupta, M. C. Deshpande, and S. P. Schwendeman. Biodegradable poly(lactic-co-glycolic acid) microparticles for injectable delivery of vaccine antigens. *Adv. Drug Deliv. Rev.* **57**:391–410 (2005).
41. I. Jabbal-Gill, W. Lin, P. Jenkins, P. Watts, M. Jimenez, L. Illum, S. S. Davis, J. M. Wood, D. Major, P. D. Minor, X. Li, E. C. Lavelle, and A. G. Coombes. Potential of polymeric lamellar substrate particles (PLSP) as adjuvants for vaccines. *Vaccine* **18**:238–250 (1999).
42. Z. Cui, and R. J. Mumper. Microparticles and nanoparticles as delivery systems for DNA vaccines. *Crit. Rev. Ther. Drug Carrier Syst.* **20**:103–137 (2003).
43. S. P. Kasturi, K. Sachaphibulkij, and K. Roy. Covalent conjugation of polyethyleneimine on biodegradable microparticles for delivery of plasmid DNA vaccines. *Biomaterials* **26**:6375–6385 (2005).
44. B. Ensoli. Rational vaccine strategies against AIDS: Background and rationale. *Microbes Infect.* **7**:1445–1452 (2005).
45. B. Ensoli. Criteria for selection of HIV vaccine candidates-general principles. *Microbes Infect.* **7**:1433–1435 (2005).
46. B. Ensoli. Introduction: Rational vaccine strategies against AIDS. *Microbes Infect.* **7**:1385 (2005).
47. G. Otten, M. Schaefer, C. Greer, M. Calderon-Cacia, D. Coit, J. Kazzaz, A. Medina-Selby, M. Selby, M. Singh, M. Ugozzoli, J. zur Megede, S. W. Barnett, D. O'Hagan, J. Donnelly, and J. Ulmer. Induction of broad and potent anti-human immunodeficiency virus immune responses in rhesus macaques by priming with a DNA vaccine and boosting with protein-adsorbed polylactide coglycolide microparticles. *J. Virol.* **77**:6087–6092 (2003).
48. J. Kreuter, R. Mauler, H. Gruschkau, and P. P. Speiser. The use of new polymethylmethacrylate adjuvants for split influenza vaccines. *Exp. Cell Biol.* **44**:12–19 (1976).
49. J. Kreuter, and P. P. Speiser. New adjuvants on a polymethylmethacrylate base. *Infect. Immun.* **13**:204–210 (1976).
50. J. Kreuter, and P. P. Speiser. *In vitro* studies of poly(methyl methacrylate) adjuvants. *J. Pharm. Sci.* **65**:1624–1627 (1976).
51. R. Q. Frazer, R. T. Byron, P. B. Osborne, and K. P. West. PMMA: An essential material in medicine and dentistry. *J. Long Term Eff. Med. Implants* **15**:629–639 (2005).
52. G. Lemperle, V. B. Morhenn, V. Pestonjamasp, and R. L. Gallo. Migration studies and histology of injectable microspheres of different sizes in mice. *Plast. Reconstr. Surg.* **113**:1380–1390 (2004).
53. G. Borchard, and J. Kreuter. Interaction of serum components with poly(methylmethacrylate) nanoparticles and the resulting body distribution after intravenous injection in rats. *J. Drug Target* **1**:15–19 (1993).
54. G. Borchard, and J. Kreuter. The role of serum complement on the organ distribution of intravenously administered poly (methyl methacrylate) nanoparticles: Effects of pre-coating with plasma and with serum complement. *Pharm. Res.* **13**: 1055–1058 (1996).
55. J. D. Watkins, S. Lancelot, G. R. Campbell, D. Esquieu, J. de Mareuil, S. Opi, S. Annappa, J. P. Salles, and E. P. Loret. Reservoir cells no longer detectable after a heterologous SHIV challenge with the synthetic HIV-1 Tat Oyi vaccine. *Retrovirology* **3**:8 (2006).
56. X. Liang, D. R. Casimiro, W. A. Schleif, F. Wang, M. E. Davies, Z. Q. Zhang, T. M. Fu, A. C. Finnefrock, L. Handt, M. P. Citron, G. Heidecker, A. Tang, M. Chen, K. A. Wilson, L. Gabryelski, M. McElhaugh, A. Carella, C. Moyer, L. Huang, S. Vitelli, D. Patel, J. Lin, E. A. Emini, and J. W. Shiver. Vectored Gag and Env but not Tat show efficacy against simian-human immunodeficiency virus 89.6P challenge in Mamu-A*01-negative rhesus monkeys. *J. Virol.* **79**:12321–12331 (2005).
57. T. Matano, M. Kano, A. Takeda, H. Nakamura, N. Nomura, Y. Furuta, T. Shioda, and Y. Nagai. No significant enhancement of protection by Tat-expressing Sendai viral vector-booster in a macaque AIDS model. *Aids* **17**:1392–1394 (2003).
58. P. Silvera, M. W. Richardson, J. Greenhouse, J. Yalley-Ogunro, N. Shaw, J. Mirchandani, K. Khalili, J. F. Zagury, M. G. Lewis, and J. Rappaport. Outcome of simian-human immunodeficiency virus strain 89.6p challenge following vaccination of rhesus macaques with human immunodeficiency virus Tat protein. *J. Virol.* **76**:3800–3809 (2002).
59. F. Titti, A. Cafaro, F. Ferrantelli, A. Tripiciano, S. Moretti, A. Caputo, R. Gavioli, F. Ensoli, M. Robert-Guroff, and B. Ensoli, Problems and emerging approaches in HIV/AIDS vaccine development. *Expert Opinion on Emerging Drugs* **12**:23–48 (2007).
60. P. Mooij, and J. L. Heeney. Rational development of prophylactic HIV vaccines based on structural and regulatory proteins. *Vaccine* **20**:304–321 (2001).
61. R. Gavioli, E. Gallerani, C. Fortini, M. Fabris, A. Bottoni, A. Canella, A. Bonaccorsi, M. Marastoni, F. Micheletti, A. Cafaro, P. Rimessi, A. Caputo, and B. Ensoli. HIV-1 tat protein modulates the generation of cytotoxic T cell epitopes by modifying proteasome composition and enzymatic activity. *J. Immunol.* **173**:3838–3843 (2004).
62. J. Zhao, R. Voltan, B. Peng, A. Davis-Warren, V. S. Kalyanaraman, W. G. Alvord, K. Aldrich, D. Bernasconi, S. Butto, A. Cafaro, B. Ensoli, and M. Robert-Guroff. Enhanced cellular immunity to SIV Gag following co-administration of adenoviruses encoding wild-type or mutant HIV Tat and SIV Gag. *Virology* **342**:1–12 (2005).